Thermal performance of ecosystems: Modeling how physiological responses to temperature scale up in communities

Camille Febvre, Colin Goldblatt, & Rana El-Sabaawi

2024

Faculty of Science

Faculty Publications

© 2024 Febvre, Goldblatt, & El-Sabaawi. This is an open access article distributed under the terms of the Creative Commons CC-BY 4.0
License: https://creativecommons.org/licenses/by/4.0.

Original citation:

Febvre, C., Goldblatt, C., & El-Sabaawi, R. (2024). Thermal performance of ecosystems: Modeling how physiological responses to temperature scale up in communities. *Journal of Theoretical Biology*, *585*, 111792. https://doi.org/10.1016/j.jtbi.2024.111792

Downloaded from UVicSpace Research & Learning Repository

dspace.library.uvic.ca


University of Victoria | Libraries

Journal of Theoretical Biology 585 (2024) 111792

Contents lists available at ScienceDirect

Journal of Theoretical Biology

journal homepage: www.elsevier.com/locate/yjtbi

Thermal performance of ecosystems: Modeling how physiological responses to temperature scale up in communities

Camille Febvre [a,b,*], Colin Goldblatt [a], Rana El-Sabaawi [b]

[a] School of Earth & Ocean Sciences, University of Victoria, 3600 Finnerty Road, Victoria, BC, Canada
[b] Department of Biology, University of Victoria, 3600 Finnerty Road, Victoria, BC, Canada

ARTICLE INFO

Model code and output: https://github.com/camille-e-e/TaNa-T.git, https://doi.org/10.20383/103.0924

Keywords:
Community
Thermal response
Tangled Nature model

ABSTRACT

Understanding how ecosystems respond to their environmental temperature is a major challenge. Thermodynamic constraints on species' metabolic rates are expected to affect ecosystem characteristics, but species interactions and interspecific variation in physiological thermal response curves (TRC) may obscure ecosystem-level responses to temperature. As a result, macroecological patterns related to temperature are still poorly understood.

We investigate how physiological TRC scale up to ecosystem-level thermal responses by modifying the Tangled Nature (TaNa) model, a stochastic network model of ecology and evolution. We include new parameterizations that make reproduction, death, and mutation temperature-dependent. We find that ecosystem survival probability depends on how the minimum fitness required for species survival varies with temperature. The thermal response of ecosystem survival probability is the only ecosystem property that is sensitive to interspecific variation in TRC. Species richness scales up directly from the TRC of mutation rate, and average species population sizes are inversely related to mutation rate, with Species Abundance Distributions (SADs) exhibiting more rare species in warmer temperatures. Interactions between species are also inversely related to mutation, with positive interactions occurring more frequently in colder temperatures. The abundance of surviving ecosystems is not sensitive to temperature. This work helps clarify the specific relationships between physiological responses to temperature and ecosystem-level repercussions when species are interacting and adapting to their thermal environments.

1. Introduction

Understanding how temperature affects ecosystems is crucial to facing major challenges of the 21st century such as combating the biodiversity crisis (Butchart et al., 2010; Cowie et al., 2022); understanding the impact of climate change on biodiversity, biomass, and ecosystem functions (e.g. Rosenzweig et al., 2008; Tittensor et al., 2021; Qin et al., 2022); and projecting the ways that ecosystem responses to climate change may feedback on the climate and other aspects of the environment (e.g. Moorcroft, 2006; Peters et al., 2013; Odling-Smee et al., 1996; Lewontin and Levins, 1997; Day et al., 2003; Laland, 2004; Lenton and Watson, 2000; Eichenseer et al., 2019; Braghiere et al., 2019). Furthermore, building an understanding of ecological responses to the environment improves our ability to interpret the history and dynamics of life on Earth recorded in the fossil record, with implications for the past, present, and future (McGill et al., 2006). However, measuring and predicting the responses of ecosystems to their environments is a major challenge (Walther, 2010; Ezard et al., 2011; Moorcroft, 2006) because different species in a shared ecosystem may respond differently to temperature (e.g. Chen et al., 2022), and the fitness of coexisting species are often directly or indirectly intertwined, making it difficult to predict the response of even a single species in the context of an ecosystem (Odling-Smee et al., 1996; Kordas et al., 2011; Guimarães et al., 2017; Bailey, 2012; Strona and Bradshaw, 2022; Remolina-Figueroa et al., 2022; Remke et al., 2022; Allsup et al., 2023).

Similar thermal responses can be observed from the scale of molecules to organisms. Metabolic rates of almost every species on Earth increase approximately exponentially with temperature, peak, and then decline more steeply than they increased (Farrell, 2016; Rezende and Bozinovic, 2019; Arroyo et al., 2022). Thermal Response Curves (TRC) of various measures of performance, such as running or swimming speed, also commonly follow this typical shape (Rezende and Bozinovic, 2019; Dell et al., 2011). Many physiological rates are

* Corresponding author at: School of Earth & Ocean Sciences, University of Victoria, 3600 Finnerty Road, Victoria, BC, Canada.
E-mail address: cfebvre@uvic.ca (C. Febvre).

https://doi.org/10.1016/j.jtbi.2024.111792
Received 11 October 2023; Received in revised form 20 February 2024; Accepted 10 March 2024
Available online 19 March 2024
0022-5193/© 2024 The Author(s). Published by Elsevier Ltd. This is an open access article under the CC BY license (http://creativecommons.org/licenses/by/4.0/).

temperature-dependent as well; birth rates show the typical hump-shaped response to temperature (Amarasekare and Savage, 2012), while death (Amarasekare and Savage, 2012) and mutation rates (Gillooly et al., 2005) increase exponentially with temperature.

Temperature also affects ecological properties and processes. Species richness generally decreases from the equator to the poles in a pattern called the Latitudinal Diversity Gradient (LDG), and the strength of the LDG is correlated with equator-to-pole temperature gradients (Brodie and Mannion, 2022). Analysis of the fossil record suggests that temperature is correlated with speciation and diversification rates (Ezard et al., 2011), and that dispersal of species has been limited by the strength of global-scale temperature gradients (Griffin et al., 2022). Some studies also suggest that interaction strengths (Dell et al., 2011) and connectance between species in ecological networks (Yuan et al., 2021) may increase with increasing temperature. Contemporary global warming has caused numerous detectable changes to ecosystems (Walther, 2010), and is predicted to decrease ocean biomass in the next decades and centuries (Jones et al., 2014). However, the ways temperature impacts ecology are much less certain than the impacts of temperature on individual organisms (Dell et al., 2011; Walther, 2010), and the extent and mechanisms by which individual-level thermal responses are responsible for producing ecosystem-level thermal responses also remains unclear.

The Metabolic Theory of Ecology (MTE) posits that biological rates from the scale of molecules to ecosystems are mechanistically linked via metabolism (Gillooly et al., 2001; Allen et al., 2002; Brown et al., 2004). The TRC of metabolism are explained by the Arrhenius–Boltzmann equation:

$$r = e^{-\mathrm{E_a}/kT} \tag{1}$$

(where r is the rate of metabolic reactions, E_a is activation energy, k is the Boltzmann constant, and T is temperature). At organismal- and population-levels, many biological rates have the same average activation energy as that of either metabolism (for rates that increase with temperature) or protein denaturation (for rates associated with death or the declining portion of hump-shaped TRC; Dell et al., 2011; Amarasekare and Savage, 2012), suggesting that metabolism and protein denaturation drive many processes from physiological to ecological scales (Brown et al., 2004). For example, MTE predicts that birth and death rates depend on metabolism (Brown et al., 2004; Price et al., 2010), leading to temperature-dependence of intrinsic growth rates of species (Price et al., 2010; Amarasekare and Savage, 2012). Species population sizes are predicted to decrease exponentially with increasing temperature as a result of the increasing metabolic requirements of each individual at warmer temperatures (Brown et al., 2004; Price et al., 2010). Furthermore, MTE suggests that patterns in species richness such as the LDG may be described by the Arrhenius equation (Allen et al., 2002). Ecosystem abundance (the total number of individuals in an ecosystem) is assumed in some studies to follow the same trend as the population sizes of constituent species (Price et al., 2010), while others have assumed it to be temperature-invariant (e.g. supported by data on trees; Allen et al., 2002). However, the thermal response of abundance has received less attention than other ecosystem metrics (e.g. Wilkinson, 2007), partially because measuring this thermal response requires large amounts of data (He et al., 2019), which can be difficult (and abstract) to measure. Controlling for bodymass, biomass is often treated similarly to population or abundance (Price et al., 2010), but understanding the thermal response of biomass additionally requires measuring and controlling for resource availability, posing another challenge to measuring the thermal response of this ecosystem metric (Price et al., 2010).

Empirical studies have provided mixed support for general relations between ecological characteristics and temperature. Data on mean activation energies of metabolism, physiological rates, performance rates, and interaction-related activities are only near the mean activation energy of metabolism when comparing species from very different environments or species of very different mass; variability increases considerably when comparing species from similar temperatures or of similar sizes (Tilman et al., 2004). In a review of the rates of activities associated with ecological interactions (such as attack or escape velocity), it was found that the average activation energies were near that of metabolism, supporting MTE predictions about interactions, but variability of activation energies for a variety of biological rates was found to increase from organismal to ecological levels (Dell et al., 2011). Measurements of species richness have produced a wide range of activation energies — not always the metabolic value predicted by MTE (Stegen et al., 2009).

Some ambiguity in empirical tests of MTE arises because the effects of temperature are difficult to separate from many other internal and external variables in empirical observations (e.g. Huete-Stauffer et al., 2015; Irlich et al., 2009), posing challenges to reconciling theory with data. Additionally, interactions between species may play an important role in determining speciation, extinction, and diversification rates, and thereby obscure the effects of temperature (Ezard et al., 2011). Interspecific variation in TRC within ecosystems may also obscure patterns in ecosystem-level thermal response (Tilman et al., 2004; Stegen et al., 2009; Isaac et al., 2012). Indeed, modeling suggests that interspecific variation may impact ecosystem biomass structure (Bideault et al., 2021) and growth rates (Chen, 2022), and may decrease the thermal dependence of species richness (Stegen et al., 2009). Consequently, it remains unclear how biological responses propagate from organismal to ecosystem scales, and what layers of complexity obscure ecosystem-level thermal responses.

In this study, we incorporate MTE and TRC into the Tangled Nature (TaNa) model of ecology and evolution (Christensen et al., 2002) to examine the propagation of physiological TRC to ecological properties that arise on geological timescales. We additionally investigate the effects of interspecific variation in species' optimal temperature of reproduction; a commonly used proxy for species fitness (Amarasekare and Savage, 2012). The TaNa model has been modified for temperature dependence before: Arthur and Nicholson (2023) scaled species fitness with temperature in the TaNa model by giving species an arbitrary, symmetrical hump-shaped TRC for interactions. Arthur and Nicholson (2023) focused on emergent feedbacks between species and climate, so ecosystem thermal responses were not expounded upon, and the paper did not incorporate any elements of MTE. Here, we integrate ecological theory into the TaNa model to investigate the mechanisms of scaling up thermal responses and the effects of diverse thermal optima. Our study additionally complements the work done by Stegen et al. (2009), in which a model developed by Loeuille and Loreau (2005) was modified to incorporate MTE principles, with the aim of explaining the variety of activation energies that have been measured for species richness. The model used by Stegen et al. (2009) is similar to the TaNa model: both define abstract species by a few traits (rather than representing specific species living on Earth), allow random mutations to produce new random species, and represent evolutionary timescales. The simplicity and long timescales of both models make them well-suited to testing MTE since MTE seeks patterns shared by distinct species and ecosystems and assumes that species have had time to adapt to their environments (Price et al., 2010). The major difference between the TaNa model and the model used by Stegen et al. (2009) is that the TaNa model does not consider bodymass or trophic levels, which enables us to isolate the temperature component of MTE and minimize constraints on species interactions in our investigation. We also broaden the focus to investigate how physiological responses to temperature scale up to a variety of ecosystem thermal responses: ecosystem survival probability, abundance, species richness, species populations sizes and distributions, and interspecific interactions. This allows us to analyze how the physiological assumptions of MTE scale up to ecosystem-level properties if all species responded to temperature in the same way, and to investigate the extent to which interspecific variation in thermal optima obscures these responses.

2. Description of the Tangled Nature model

2.1. General properties

The TaNa model is a mathematical model of ecology and evolution (Christensen et al., 2002). Ecology is represented by interactions between species which affect specific reproduction rates, and evolution is enabled by allowing mutations to produce new species. The model was originally developed to capture the dynamics of Punctuated Equilibria, a widely observed pattern in the fossil record in which species morphology remains relatively constant over long periods of time (tens of thousands to tens of millions of years), and then changes in rapid bursts associated with changes in the biotic or abiotic environment experienced by species (Gould and Eldredge, 1977).

Stochasticity in the TaNa model causes every model realization to follow a different trajectory, but Punctuated Equilibria always emerge: the abundance of model communities fluctuates around the same mean for long periods called quasi-stable states, until the state is interrupted by an abrupt transitional period, called a quake, and a subsequent change in mean abundance, which is then maintained in the next quasi-stable state (Fig. A.11). During quasi-stable states, ecological communities are dominated by just a few "core" species, defined as the most populous species and all other species with populations at least 10% as large. The rest of the species, with relatively small populations, are called "cloud" species.

Punctuated Equilibria arise in the TaNa model purely as a result of the interactions between species: positive interactions between core species stabilize the community in quasi-stable states, and these are only occasionally disrupted by mutant species with parasitic effects on core species (Arthur et al., 2017). Parameters are chosen in the model to reproduce the characteristic distribution of species populations (called Species Abundance Distributions, SADs) observed in real ecosystems (McGill et al., 2007), such that during quasi-stable states, the majority of the population is in the core and the majority of the species richness is made up of cloud species (Anderson and Jensen, 2005).

2.2. Properties and operation of the TaNa model

Each TaNa model simulation is initialized with $D_0 = 60$ random species. The initial abundance ($N_0 = 500$) of individuals in the ecosystem is equally distributed between the species (some randomly selected species have one more initial individual than others to avoid fractional populations). Species are defined by binary numbers of $L = 20$ bits (allowing the potential for $2^L = 1,048,576$ distinct model species in each simulation).

In each timestep (t), $N(t)$ individuals are sequentially selected randomly with replacement. For each selected individual, a random number is drawn between 0 and 1, and if the number is smaller than the death probability ($p_{\text{death}} = 0.2$), the individual dies. If the selected individual survives, another random number is drawn, and the individual reproduces if the number is smaller than its reproduction probability ($p_{\text{off,f}}$, which depends on its fitness, explained below). If the individual reproduces, L more random numbers are drawn, and for each random number below the mutation probability ($p_{\text{mut}} = 0.01$), a bit in the species-specific binary number flips, giving the offspring a new binary number and thus a new species identity. As the evolutionary dynamics of the TaNa model represent geological timescales, it is assumed that each mutant species has already sufficiently diverged from the ancestral species to fill a new ecological niche (such that new interactions with the other species in the ecosystem have evolved).

The reproduction probability of each species i depends on its fitness (f_i) :

$$p_{\text{off,f}}(f_i, t) = \frac{1}{1 + e^{-f_i(t)}}, \tag{2}$$

Table 1
Parameters in the TaNa and TaNa+T models are the same in every simulation of the same temperature (in the TaNa+T, we make the values of $p_{\text{off,T}}$, p_{death}, and p_{mut} depend on the temperature of simulations). Constants are randomly assigned at the beginning of each simulation. State variables change over time. Functions relate model quantities with other variables.

TaNa model parameters (and their value in the original TaNa model)	
$p_{\text{off,T}}$	Temperature-dependent scaler of reproduction probability (1).
p_{death}	Probability of an individual dying in a timestep (0.2).
p_{mut}	Probability (per bit) of mutation during reproduction (0.01).
μ	Damping coefficient on population growth (0.2).
L	Number of bits in species' identifying binary numbers (20).
C	Scale of interactions between species (100).
θ	Fraction of species pairs that have interactions (0.25).
Randomly assigned constants	
J_{ij}	Impact of species j on species i.
State variables	
$N(t)$	Abundance (number of individuals in ecosystem) at time t.
$N_i(t)$	Population of species i at time t.
$D(t)$	Species richness (number of species in ecosystem) at time t.
Functions	
$f_i(t)$	Fitness of species i at time t (Eq. (3)).
$p_{\text{off,f}}(f_i, t)$	Interaction-dependent component of reproduction probability of species i at time t (Eq. (2)).
$p_{\text{off,total}}(f_i, t, T)$	Total reproduction probability of species i at time t and temperature T (Eq. (5)).

such that species with $f_i(t) = 0$ have a 50% chance of reproducing, $\lim_{f_i \to \infty} p_{\text{off,f}} = 1$, and $\lim_{f_i \to -\infty} p_{\text{off,f}} = 0$. The fitness of species i at time t is determined by its interactions with each other species j:

$$f_i(t) = -\mu N(t) + \sum_{j=1}^{D(t)} J_{ij} \frac{N_j(t)}{N(t)}, \tag{3}$$

where μ is a damping factor (representing ecological resource constraints) that limits growth of each species in proportion to the abundance ($N(t)$) of the ecosystem, $D(t)$ is the species richness (number of extant species) at time t, J_{ij} is the effect of species j on species i, and $N_j(t)$ the population of species j at time t.

The interactions between species are prescribed from the interaction matrix (**J**), made up of random numbers J_{ij} drawn from a product normal distribution centered at zero and for which each normal distribution has a standard deviation of $C = 100$. The leading diagonal of the matrix is set to zero ($J_{\text{ii}} = 0$), such that organisms cannot have ecological interactions with members of their own species (other than through density-dependence, which is included at the ecosystem-level through the negative μ term in Eq. (3)). A fraction $1 - \theta$ of the elements in matrix **J** are set to zero, representing species pairs that do not interact at all. Connectance (θ) is set to 0.25 to produce realistic SADs in the model (Anderson and Jensen, 2005). TaNa model variables are summarized in Table 1.

3. Methods: TaNa+T

3.1. Temperature-dependence of physiological parameters

We modify the three physiological parameters of the TaNa model (birth, death, and mutation probabilities) to create a temperature-dependent version called the TaNa+T. To include the impact of temperature on reproduction, we use a unimodal, left-skew curve from the Python scipy toolkit (called "skewnormal" in the Scipy package; Fig. 1, red dashed line). This curve can be shifted to any temperature without changing shape. It is parameterized to match the general TRC for reproduction rate ($r_{\text{off}}(T)$) derived in Amarasekare and Savage (2012) (the second term in Eq. 11 of that paper; Fig. 1, black solid line), and the parameters we used in that equation are listed in Appendix B.

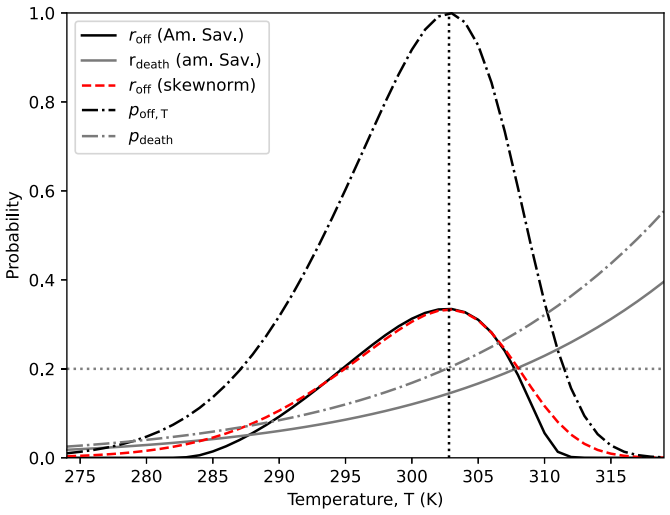

Fig. 1. Birth rate (r_{off}, solid black line; Eq. (B.1)) and the skewnormal curve we used to approximate it (red dashed line), and death rate (r_{death}, solid gray line), from Amarasekare and Savage (2012) (parameter values listed in Appendix B). We scale the red-dashed line to have a maximum of 1 for reproduction probability ($p_{off,T}$, black dot-dashed line), and scale r_{death} to the control value of death probability (0.2; horizontal dotted line) at the control temperature (T_{ctrl}) for death probability ($p_{death,T}$, gray dot-dashed line). The vertical dotted line shows T_{ctrl} = 303 K ≈ 30 °C). Temperature is reported in Kelvin, ranging from about 1 °C at 274 K to 47 °C at 320 K.

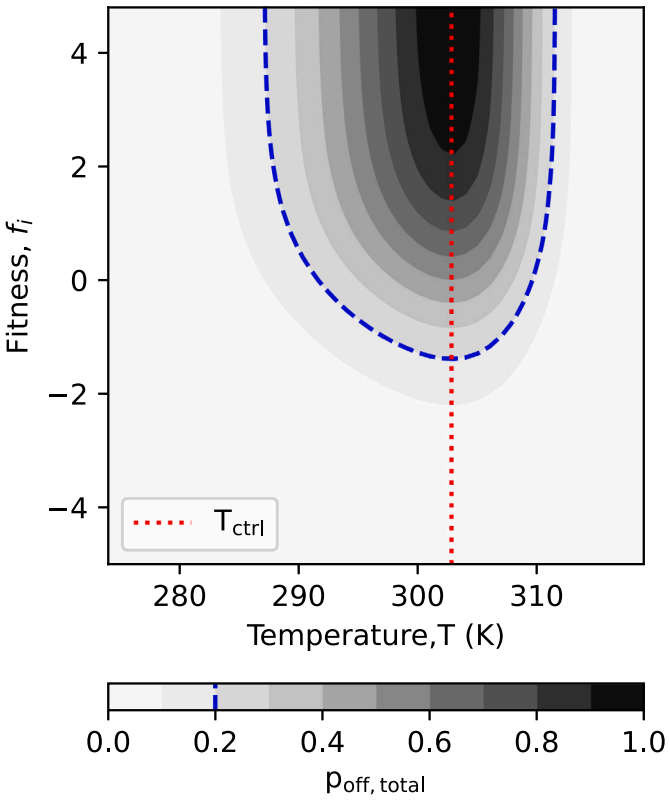

Fig. 2. Reproduction probability ($p_{off,total}$; Eq. (5)) as a function of temperature (T; horizontal axis) and fitness (f_i; vertical axis). The dotted red line shows the control temperature (T_{ctrl} = 303 K; at which $p_{death}(T_{ctrl}) = 0.2$ and $p_{off,T}(T_{ctrl}) = 1$). The dashed blue contour shows $p_{off,total} = 0.2$, the minimum $p_{off,total}$ required for a species to survive at T_{ctrl}. Note that at a fixed temperature, the fitness of a species depends on ecosystem abundance (N) and the relative abundances of other species (n_j; see Eq. (2)), so $p_{off,total}(i,t,T)$ varies between species and over time.

The TaNa model uses probabilities to determine which individuals die, reproduce, and mutate (rather than prescribing population-level rates), so we scale $r_{off}(T)$ to have a maximum of 1 (using a scaling factor of 3.0), giving a temperature-dependent reproduction probability with a peak at T_{opt}:

$$p_{off,T} \propto r_{off}(T) \tag{4}$$

(Fig. 1, black dot-dash line), and we make $T_{opt} = 303K(\approx 30^oC)$ the control temperature (T_{ctrl}; Fig. 1, black dotted line). The combined effect of both temperature and fitness on reproduction probability is then modeled as

$$p_{off,total}(f_i,t,T) = p_{off,T}(T)p_{off,f}(f_i,t), \tag{5}$$

where $p_{off,total}$ is the temperature- and fitness-dependent reproduction probability (Fig. 2).

The temperature dependence of death probability is modeled in the form of the Arrhenius–Boltzmann equation:

$$p_{death}(T) = d_0 \exp\left(-E_a/(kT)\right), \tag{6}$$

where d_0 is a scaling factor and E_a is the activation energy of death (set to E_a = 0.49 eV) (Amarasekare and Savage, 2012). We set $d_0 = 8.17\times10^7$ such that the value of death probability at T_{ctrl} is the same as in the original TaNa model ($p_{death}(T_{ctrl}) = 0.2$) (Fig. 1, 3).

The temperature dependence of mutation probability (p_{mut}) also takes the form of the Arrhenius–Boltzmann equation:

$$p_{mut}(T) = m_0 \exp\left(-E_a/(kT)\right), \tag{7}$$

where m_0 is a scaling factor (set to 3.58×10^6 so $p_{mut}(T_{ctrl}) = 0.01$; the control value) (Gillooly et al., 2005; Stegen et al., 2009) (Fig. 3). Although the form of p_{death} and p_{mut} is exponential, the values of p_{death} and p_{mut} realized in the TaNa+T (for T between 274 K and 320 K) do not approach 1, so we do not modify the equations to saturate at 1.

3.2. Experimental set-up

We perform in silico experiments with three model configurations to: (1) explore the effects of each of the three physiological parameters on the model generally ("parameter exploration"; 50 simulations at each parameterization); (2) investigate ecological response to temperature without the complication of thermal diversity ("single-TRC" experiment; 250 simulations at each temperature); and (3) examine the effects of interspecific variation in TRC on ecological response to temperature ("various-TRC" experiment; 250 simulations at each temperature). All simulations are run for 10,000 generations.

In the parameter exploration, we examine the effects of reproduction, death, and mutation probabilities on the model without linking their values to temperature. Although the term we use to scale the interaction-dependent component of reproduction is not associated with temperature in the parameter exploration, we still refer to it as $p_{off,T}$ for consistency with Eq. (5) and with the temperature-dependent sections. We vary both $p_{off,T}$ and p_{death} from 0.1 to 1 along intervals of 0.1, (while allowing $p_{off,f}$ to emerge in the model as usual). This parameter range includes the control values of reproduction ($p_{off,T}$ = 1) and death (p_{death} = 0.2) and also ranges across all possible probabilities. We linearly vary mutation probability from 0.004 to 0.019 along intervals of 0.003. One-dimensional explorations of the other parameters in the model are reported in Appendix C. Fifty simulations were run at each parameterization.

In "single-TRC" experiments, $T_{opt} = T_{ctrl}$, so all species have identical TRCs for reproduction, death, and mutation probabilities (Fig. 3a). We run 250 single-TRC experiments at each constant temperature between 274 K and 320 K (≈ 1–47 °C; the range of temperatures in which most species live; Gillooly et al., 2001) in intervals of 3 K. Single-TRC experiments simplify the scaling up of thermal response from a single species to a community, and isolate the effects of ecological

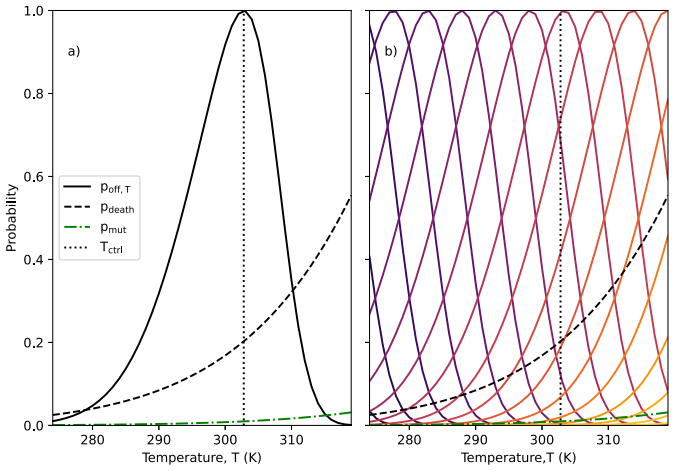

Fig. 3. The experimental set-ups of (a) single-TRC and (b) various-TRC experiments. Solid lines show reproduction probabilities; several example TRC are shown for various-TRC experiments (colors in panel (b)). Black dashed lines show death probability (p_{death}); the same exponential curve in both setups. Green dot-dashed lines show mutation probability (p_{mut}) in both experimental set-ups. The vertical black dotted line shows the control temperature (T_{ctrl}), at which all TaNa+T parameters correspond to those used in the original TaNa model.

interactions on affecting community-level thermal response, enabling us to investigate how thermal response propagates from the individual to the ecosystem in a scenario without interspecific variation in thermal preferences. These experiments also set a baseline to which results from more complicated evolutionary set-ups can be compared, and the similarities and differences between the idealized and more realistic cases provide insight into the effects of evolution on community response to temperature.

In "various-TRC" experiments, we allow the optimal temperature (T_{opt}) of reproduction to vary between species (Fig. 3b). These simulations enable species to adapt to their environment, and species experience selective pressures both due to temperature-adaptation and to species interactions. In various-TRC simulations, species-specific T_{opt} values ($T_{opt,i}$) are drawn from a uniform distribution between 263 and 330 K (−10 and 53 °C) — extending above and below the temperature range at which experiments are run in order to minimize edge-effects. 250 various-TRC simulations are run at each constant temperature between 274 K and 320 K in intervals of 3 K.

4. Results

We first present the results of the parameter exploration (Section 4.1), in which we vary the temperature-dependent component of reproduction probability ($p_{off,T}$), death probability (p_{death}), and mutation probability (p_{mut}) in the same way for all species. We then present the results of the temperature-dependent TaNa model (TaNa+T), in which each temperature corresponds to a specific value of p_{death} and p_{mut} (Section 4.2). Section 4.2 includes the results for both single-TRC experiments (in which $T_{opt} = T_{ctrl}$ for all species) and various-TRC experiments (in which species have different thermal optima of reproduction ($T_{opt,i}$)).

We analyze ecosystem-level responses to temperature based on five different ecosystem characteristics all measured at the end of the 10,000 generation simulations. The section on temperature-dependence of the TaNa model (Section 4.2) is broken down into subsections corresponding to each of these five model outputs. Ecosystem survival probability is the fraction of experiments in which any organisms exist at the end of the simulation. Abundance is the total number of individuals in the ecosystem. Species richness is the number of species in the ecosystem. SADs are distributions of species populations. Interactions are the J_{ij} values of surviving organisms in ecosystems.

4.1. Parameter exploration

In the simulations presented in this section, parameters are varied independently from each other, and reproduction ($p_{off,T}$), death (p_{death}), and mutation (p_{mut}) probabilities are not associated with temperature.

In the parameter exploration, we find that ecosystem survival probability is positively correlated with $p_{off,T}$ and inversely correlated with p_{death} (Fig. 4, top row). No ecosystems survive if $p_{off,T} < p_{death}$ because no species could survive with $p_{off,total} < p_{death}$. For $p_{off,T} < p_{death}$, ecosystem survival probability increases monotonically with $\frac{p_{off,T}}{p_{death}}$ (Fig. 5).

The slope of increase in ecosystem survival probability relative to $\frac{p_{off,T}}{p_{death}}$ depends on mutation probability (Fig. 5). Smaller values of p_{mut} increase ecosystem survival probability in harsher conditions (when $p_{off,T}$ is near p_{death}), but also decrease the rate at which ecosystem survival probability increases relative to $\frac{p_{off,T}}{p_{death}}$; consequently, larger values of $\frac{p_{off,T}}{p_{death}}$ are required before ecosystem survival probability finally reaches 1 when p_{mut} is small. At larger mutation probabilities, a larger ratio of $\frac{p_{off,T}}{p_{death}}$ is required for ecosystem survival when $p_{off,T}$ is close to p_{death}, but ecosystem survival probability then increases more steeply and reaches 1 at smaller $\frac{p_{off,T}}{p_{death}}$.

Ecosystem survival probability is indicative of the values of $p_{off,f}$ occurring in ecosystems. The distribution of $p_{off,f}$ is an emergent property in the TaNa+T: species specific values of $p_{off,f}$ depend on the random interactions between species, leading to selection on species depending on their interactions. Survival of any species requires $p_{off,total} > p_{death}$ for that species, and using $p_{off,total} = p_{off,T}p_{off,f}$ (Eq. (5)), species survival requires $\frac{p_{off,T}}{p_{death}} > \frac{1}{p_{off,f}}$. In the control case ($p_{mut} = 0.01$), ecosystem survival probability is first positive when $\frac{p_{off,T}}{p_{death}} \approx 1.2$, suggesting that $p_{off,f} > 0.83$ is very unlikely. The value of $\frac{p_{off,T}}{p_{death}}$ at which ecosystem survival probability first reaches ≈ 1 occurs when $\frac{p_{off,T}}{p_{death}} \approx 4$. As almost all ecosystems survive in these conditions, it suggests that values of $p_{off,f}$ of at least 0.25 are a common occurrence amongst mutant species outside of quasi-steady states at this mutation probability. The threshold value of $p_{off,f}$ required for ecosystem survival depends on p_{mut} (Fig. 5).

Abundance of all surviving ecosystems is not affected by $p_{off,T}$, p_{death}, or p_{mut} (Fig. 4, second row). Consequently, abundance should not be expected to vary with temperature, unless interspecific variation in TRC produces its own effect on abundance in various-TRC simulations.

Species richness increases with increasing mutation probability (Fig. 4, bottom row). It is unaffected by $p_{off,T}$ and death probability.

The impacts of all 7 model parameters are summarized in Appendix C.

4.2. Effects of temperature on the tana model

We now present our investigation of the behavior of the TaNa+T model, in which each temperature is associated with a particular value of p_{death} and p_{mut}, and $p_{off,T}$ depends on temperature and species specific values of $T_{opt,i}$.

4.2.1. Ecosystem survival probability

In TaNa+T simulations, ecosystem survival probability is temperature-dependent, with a response shape that is sensitive to interspecific variation in TRC. When all species have the same TRC (single-TRC simulations), ecosystem survival probability has a top-hat-shaped response to temperature: it is zero at temperatures below approximately 280 K (≈ 7 °C; temperatures at which $p_{death} > p_{off,T}$) and above $T \approx 310$ K (≈ 37 °C; the upper temperature at which $p_{death} > p_{off,T}$; Fig. 6a, black line), and ecosystem survival probability is near 1 between those temperatures. The shape of this thermal response is wider and more symmetrical than the TRC of reproduction.

The thermal response of single-TRC ecosystem survival probability is controlled by constraints on species-level fitness. For a species to

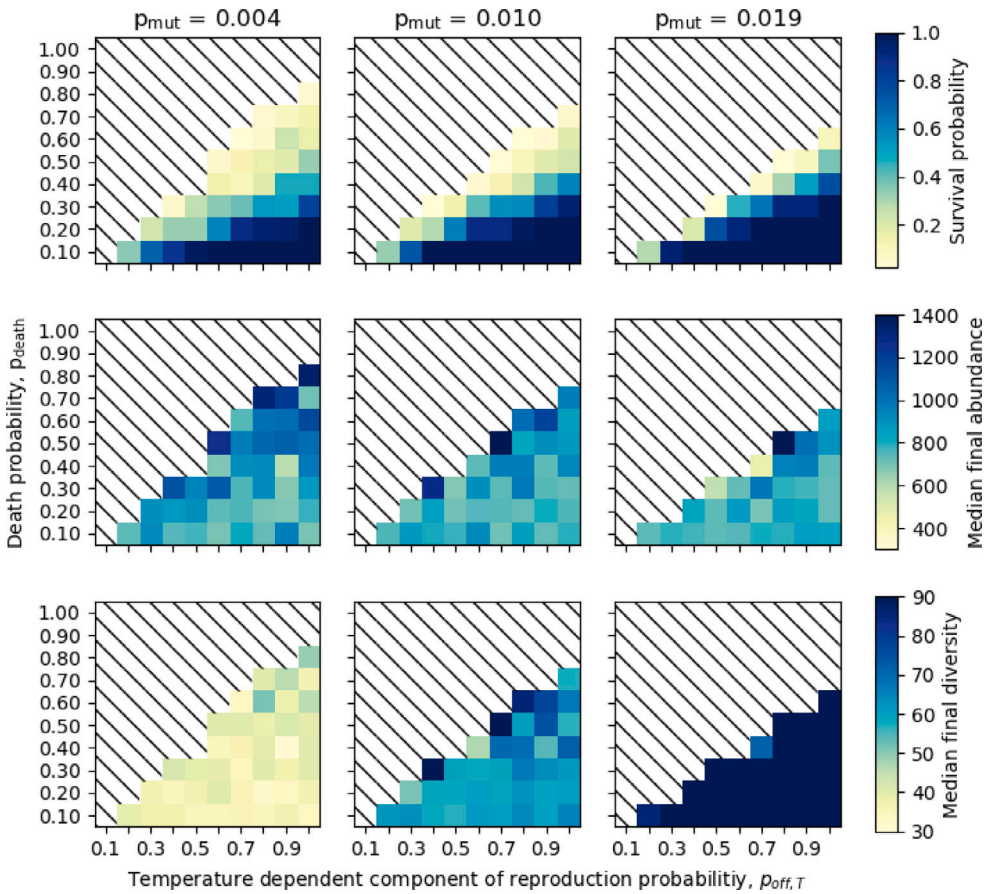

Fig. 4. Parameter exploration of the temperature-dependent component of reproduction probability ($p_{\text{off,T}}$; here not associated with temperature; horizontal axes), death probability (p_{death}; vertical axes), and mutation probability (p_{mut}; columns). Fifty TaNa model simulations were run for 10,000 generations at each parameterization. Colors of the boxes indicate the fraction of surviving experiments (top row), median abundance (middle row), and median species richness (bottom row) at the end of simulations. The hashed regions indicate parameterizations at which no simulations survived to 10,000 generations.

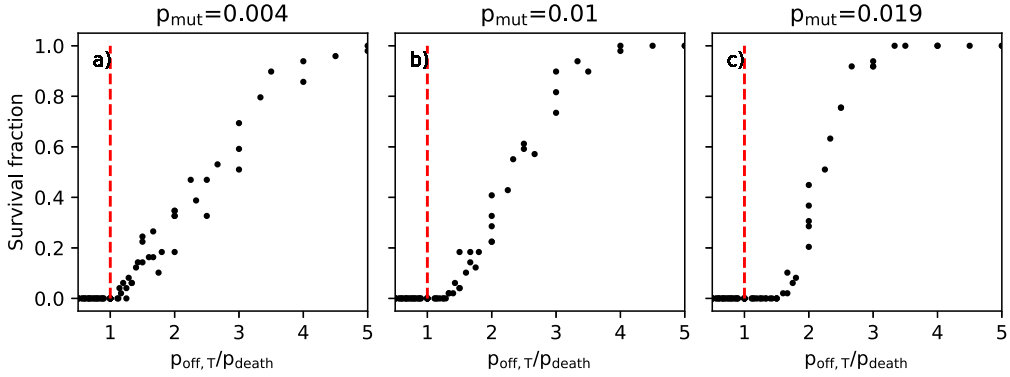

Fig. 5. The relationship between survival fraction and $\frac{p_{\text{off,T}}}{p_{\text{death}}}$ is shown for (a) $p_{\text{mut}} = 0.004$, (b) $p_{\text{mut}} = 0.01$ (control), and (c) $p_{\text{mut}} = 0.019$. The dashed red lines show $p_{\text{off,T}}/p_{\text{death}} = 1$. Values of $p_{\text{off,T}}/p_{\text{death}}$ less than 0.5 are all zero; values greater than 5 are all near 1 (not shown).

survive, its total reproduction probability ($p_{\text{off,total}}$) must be larger than its death probability (p_{death}). Substituting Eq. (5) for $p_{\text{off,total}}$ and rearranging the equation, we can see that species survival requires $p_{\text{off,f}} > \frac{p_{\text{death}}}{p_{\text{off,T}}}$. Solving for fitness ($f_i$) using Eq. (2), an individual must have a fitness

$$f_i > -\log\left(\frac{p_{\text{off,T}}}{p_{\text{death}}} - 1\right) \tag{8}$$

in order to survive. Indeed, ecosystem survival probability increases as the threshold fitness required for species survival decreases (Fig. 6a). The thermal response of ecosystem survival probability is very similar when mutation probability (p_{mut}) is held constant (Fig. 6a, red line), suggesting that mutation probability does not have a strong impact on ecosystem survival probability, and the minor effect of mutation probability can be explained by Fig. 5a from the parameter exploration.

In various-TRC experiments ($T_{\text{opt,i}}$ varies between species), the thermal response of ecosystem survival probability decreases quasi-linearly from around 0.95 at the coldest temperature to zero at the warmest temperature (Fig. 6b). The shape of the thermal response of various-TRC experiments is again determined by the threshold fitness required for species survival (Eq. (8); shown for several example $T_{\text{opt,i}}$ in the blue lines in Fig. 6b). In temperatures below 297 K, ecosystem survival probability is slightly smaller when p_{mut} varies with temperature than when

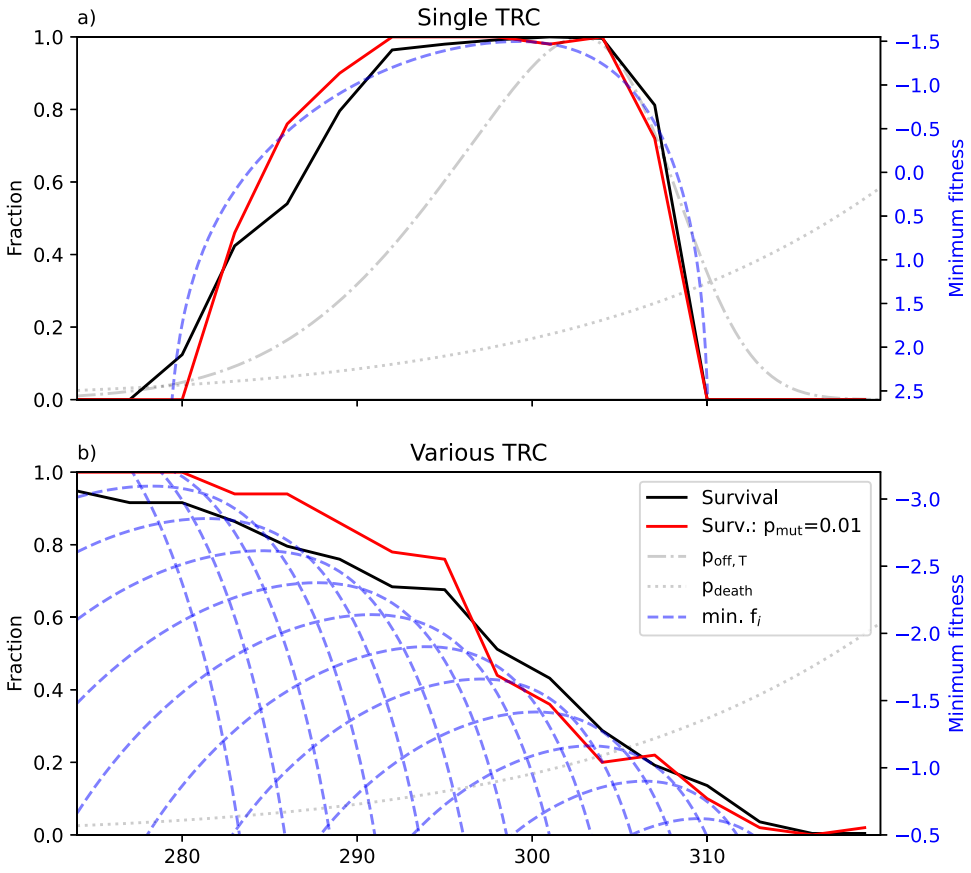

Fig. 6. (a) The fraction of surviving experiments out of 250 single-TRC TaNa+T simulations at each temperature (black), compared to the fraction of surviving ecosystems out of 50 single-TRC simulations run at each temperature with $p_{mut} = 0.01$ (red). The light gray dash-dotted and dotted lines shows the input $p_{off,T}$ and $p_{death}(T)$, respectively. The blue dashed line shows the minimum fitness required for a species to survive (Eq. (8)) at each temperature (corresponding to the vertical axis on the right, axis inverted for comparison to ecosystem survival fraction). (b) Same as for (a), but for various-TRC simulations, and the blue dashed lines in (b) show the minimum fitness threshold for several example values of $T_{opt,i}$ that various-TRC organisms could have.

it is held at $p_{mut} = 0.01$ (Fig. 6b, red line) showing that smaller values of p_{mut} still decrease large values of ecosystem survival probability when TRC vary between species (the same as when all species have the same TRC; Fig. 5). The survival fraction decreases with temperature because the maximum probability of reproduction in various-TRC experiments does not vary with temperature, whereas the probability of death does.

4.2.2. Ecosystem abundance

The abundance of individuals in surviving ecosystems, as well as their partitioning of individuals into cores and clouds, is relatively constant across temperatures, regardless of whether TRC vary between species or not (Fig. 7 a,b,g,h). This aligns with findings from Section 4.1. Additionally, as $p_{off,T}$ does not affect abundance (Fig. 4), interspecific variation in $p_{off,T}$ has no effect on abundance and the thermal response of abundance is the same in single-TRC and various-TRC simulations. Consequently, the only possibly response of abundance to temperature would be through the thermal response of ecosystem survival probability: if mean abundance was measured across both surviving and extinct ecosystems, with zeros in harsher climates driving the mean down, the thermal response of abundance would have the same shape as that of ecosystem survival probability, and abundance would therefore appear to depend on both temperature and interspecific variation in TRC (not shown).

4.2.3. Species richness

Species richness of ecosystems (the number of species) increases in warmer temperatures, whether TRC vary between species or not (Fig. 7 c,d). In Arrhenius plots, the logarithm of the response metric is plotted against $\frac{1}{kT}$, such that exponentials appear as straight lines with the slope equal to the activation energy ($-E_a$) in the Arrhenius equation (Eq. (1)). In Fig. 7 c,d, species richness indeed appears as a straight line, with a slope close to that of metabolism (blue dashed line), suggesting that the TRC of species richness scales up from metabolic processes. As shown in the parameter exploration (Section 4.1), mutation drives the thermal response of species richness in single-TRC simulations. The thermal response of species richness in various-TRC is the same because $p_{off,T}$ does not affect species richness (Section 4.1), so interspecific variation in the TRC of reproduction has no effect.

The number of core species also increases with warmer temperatures in single-TRC and various-TRC experiments; from about 2 to 4 core species in both (Fig. 7 i,j). However, the activation energy of core species richness is smaller than the metabolic value (*i.e.* the slope of core species richness in the Arrhenius plots is shallower than the blue dashed lines). This indicates that metabolic processes have a weaker impact on core species richness than on cloud species richness.

4.2.4. Population sizes and SADs

Average population sizes of species in ecosystems decrease exponentially as temperature increases in both single-TRC and various-TRC simulations (Fig. 7 e,f), while population sizes remain relatively constant across temperatures in cores (Fig. 7 k,l). The thermal response of average population size in ecosystems is driven by the thermal response of species richness (since abundance is temperature-independent), and species richness is in turn driven by the thermal response of mutation rate (Section 4.2.3). Interspecific variation in TRC does not affect the thermal response of average population sizes because it does not affect abundance or species richness.

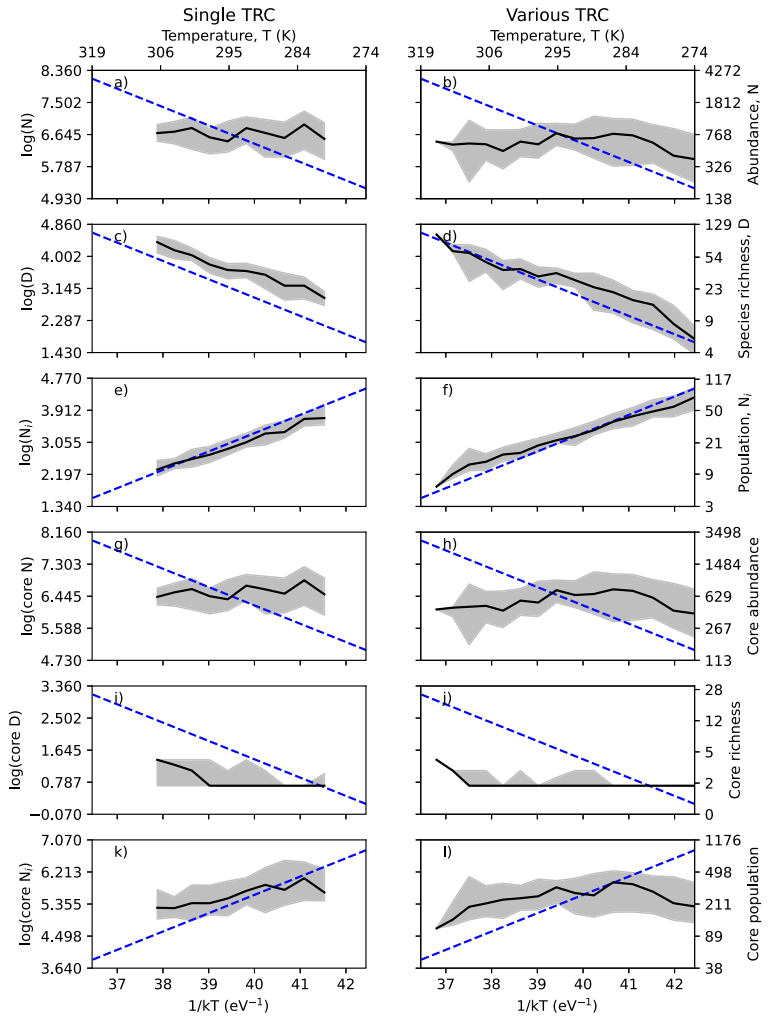

Fig. 7. Rows from top to bottom: Arrhenius plots of 1. median abundance, 2. species richness, 3. population size, 4. core abundance, 5. core species richness, and 6. core population size for single-TRC (left) and various-TRC (right) experiments (interquartile ranges in the shaded gray regions). Blue dashed lines have slopes of −0.49 eV (a–d, g–j) and 0.49 eV (e,f,k,l), showing the activation energy (E_a) of metabolism. Horizontal axes are labeled in units of Kelvin along the top, and units of $\frac{1}{kT}$ on the bottom. Vertical axes are logarithmic, with corresponding real values on the right.

All ecosystems exhibit the typical SAD shape, with the majority of the abundance made up by a few core species, and with many more cloud species than core species (Fig. 8). The shape of SADs is temperature-dependent, with increasing diversity of cloud species emerging in warmer temperatures (Fig. 8). As a result, SADs become more positively skewed as temperature increases (Fig. 9 e,f,g,h). SAD skewness is additionally correlated with both species richness and abundance (Fig. 9 a,b,c,d). In single-TRC experiments, there is no relationship between SAD skewness and abundance or species richness for ecosystems at the same temperature (no trend in colors in Fig. 9 e,f), showing that abundance and species richness do not drive SAD skewness. However, in various-TRC experiments, abundance and species richness do appear to affect skewness within each temperature (trend in colors in Fig. 9 g,h), with more abundant and more diverse ecosystems exhibiting more positive SAD skewness (more cloud species).

4.2.5. Interactions between species

In both single-TRC and various-TRC experiments, mean interactions (J_{ij}) are more positive in colder temperatures, and decrease to almost zero in the warmest temperatures (Fig. 10, black). On a linear temperature scale, core species show a clear decreasing trend in mean interaction strength relative to temperature (black dots in Fig. 10 b,d). However, Arrhenius plots show that the rate of decrease in mean interaction strengths is actually steeper in the ecosystem average than for just core species (Fig. 10, bottom row, black lines). The thermal response of mean ecosystem interactions has an activation energy near the metabolic value (E_a = 0.49 eV; Fig. 10 e,g, black dashed lines), whereas core interactions have a slightly smaller activation energy (Fig. 10 f,h). No thermal response is detectable in experiments in which p_{mut} was held constant (red dots and lines in Fig. 10), so as for species richness and average population size, the thermal response of ecosystem and core interactions is driven by the TRC of mutation ($p_{\text{mut}}(T)$).

Pairwise interactions can be categorized into five types: mutualistic (both species benefit one another), competitive (both species harm one another), predatory (one species benefits while the other is harmed), one-way positive (one species benefits without impacting the other), one-way negative (one species is harmed without impacting the other), or no interaction. The fraction of species pairs with any interactions relative to all possible interactions is the emergent connectance. In TaNa+T simulations, interaction types do not vary with temperature for ecosystems or cores in any of the simulations run (not shown). Additionally, ecosystem connectance does not evolve away from θ (the preset fraction of species that interact) for core or cloud species in any temperature (not shown). This suggests that thermal responses of interaction types and connectance do not arise from the TRC of birth, death, and mutation.

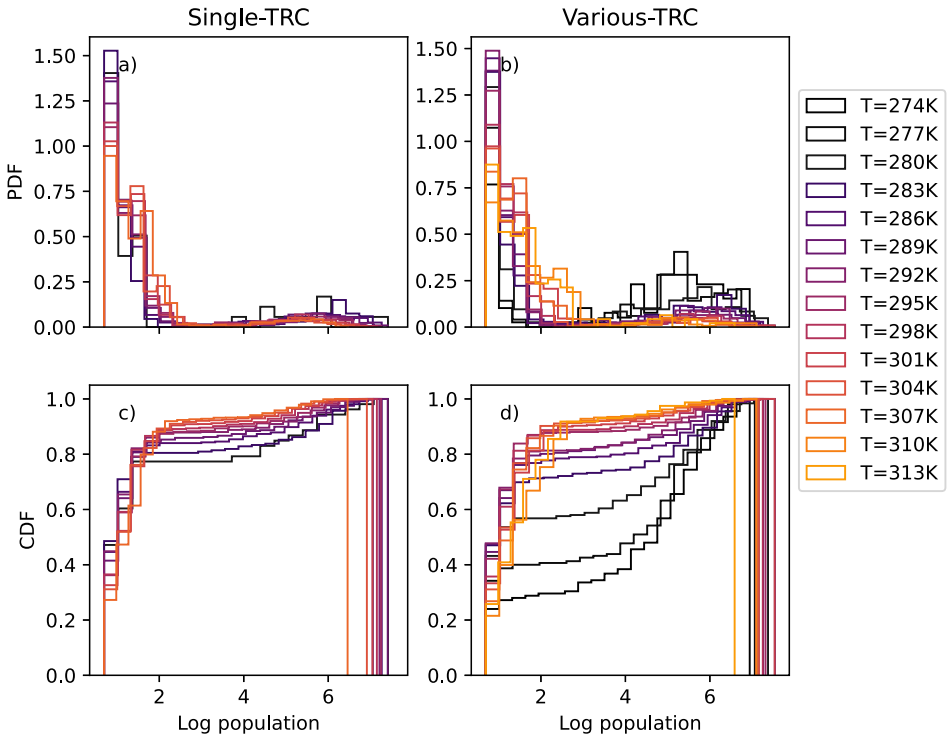

Fig. 8. Histograms plotted as Probability Density Functions (PDFs; top row) and Cumulative probability Density Functions (CDFs; bottom row) of Species Abundance Distributions (SADs) for single-TRC (left) and various-TRC (right) experiments. The bimodality of both PDFs in the top row shows the cloud (left peaks in each panel) and core species (right peaks in each panel). The CDFs exhibit the effects of temperature more clearly.

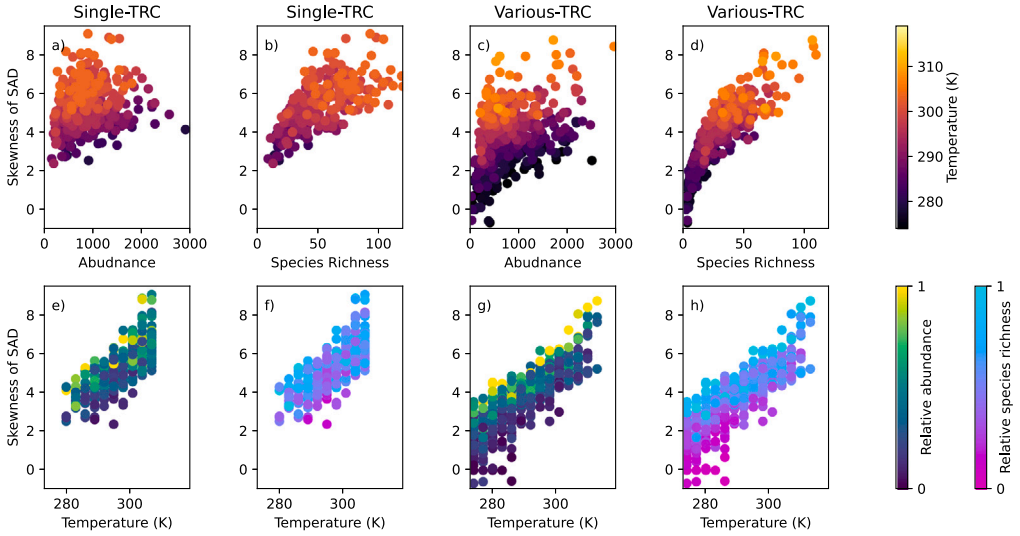

Fig. 9. Scatterplots of skewness of Species Abundance Distributions (SADs) of the logarithm of species populations relative to: (a,c) ecosystem abundance, (b,d) species richness, and (e–h) temperature. The first two columns correspond to single-TRC experiments and the last two to various-TRC. Colors in panels (a–d) correspond to the temperature of the single model runs. In panels (e) and (g), the colors at each temperature correspond to the relative abundance at that temperature, and in panels (f) and (h), the colors correspond to the relative species richness at that temperature. The information in each column is the same, with the horizontal axis and color scheme switched between rows.

5. Discussion

The primary aim of this study is to investigate how physiological TRC scale up to ecological characteristics. We find that species richness, average population size, and interaction strength all scale up in proportion or inversely proportional to mutation rate, with stronger responses from cloud than core species. Ecosystem survival probability is also sensitive to temperature, but does not scale up directly from any physiological TRC. Ecosystem abundance and interaction types are not sensitive to temperature at all. Additionally, only the thermal response of ecosystem survival probability is sensitive to interspecific variation in the optimal temperature of reproduction. These results arise from the ecological and thermal assumptions we built into the TaNa+T, and warrant further discussion.

Ecosystem survival probability is mainly controlled by the ratio between reproduction and death probabilities in single-TRC TaNa+T simulations (Fig. 5). Since that ratio is affected by interspecific variation in the TRC of reproduction, ecosystem survival probability depends on interspecific variation in TRC in TaNa+T simulations (Fig. 6). Traditionally, species fitness is often considered in terms of intrinsic growth

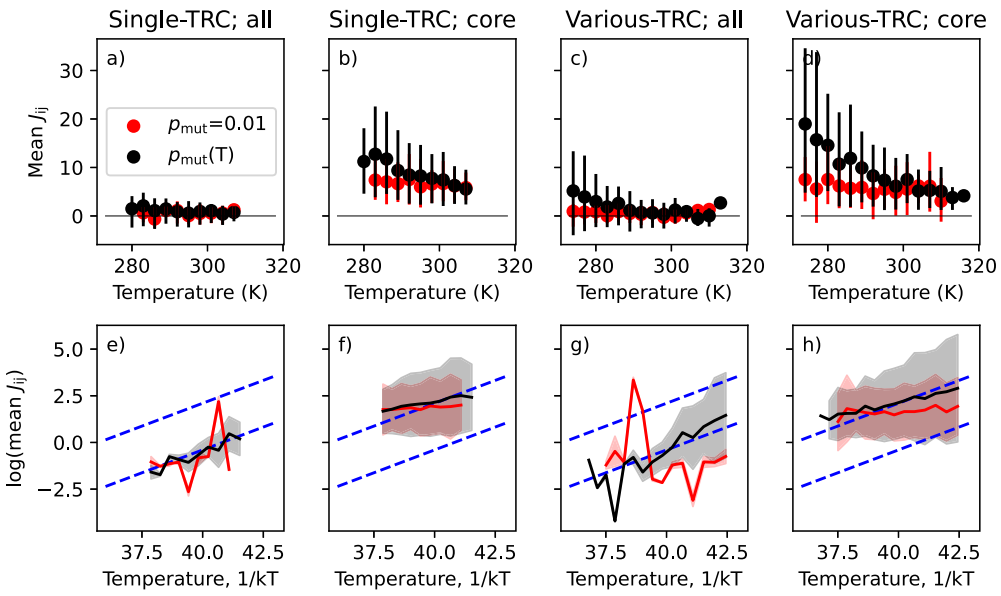

Fig. 10. Top row: Mean of within-ecosystem mean interactions (J_{ij}) for single-TRC (first two panels) and various-TRC (last two panels) between all species in the ecosystem (a,c) and between core species only (b,d). Vertical lines show the 10th to 90th percentiles. Results from 250 TaNa+T simulations at each temperature are shown in black ($p_{off,T}$, p_{death}, and p_{mut} all vary with temperature); results from 50 simulations in which p_{mut} was held constant are shown in red. Bottom row: The same information is shown on Arrhenius plots, except the shaded regions show mean ± one standard deviation. The blue dashed lines have a slope corresponding to the activation energy of metabolism ($E_a = 0.49$ eV).

rate; the difference between birth and death rates, rather than their ratio. The ratio is important in this model because the temperature-dependent response of reproduction is only one component of reproduction probability, and species survival requires that total reproduction probability (the product of two probabilities) be larger than death probability. Therefore, we suggest that more attention be paid to the ratio between reproduction and death probabilities, especially when a partial measure of reproduction rate is being studied. The specific thermal responses found for ecosystem survival probability in this study are difficult to validate, however, because ecosystem survival probability is not readily measured in the real world — the geological record is incomplete, and environments in which ecosystems failed to establish do not necessarily leave a record. Additionally, while there are clear boundaries between ecosystems in different TaNa+T simulations, ecosystems on Earth are often overlapping and lack clearly defined boundaries.

While the number of ecosystems that survive depends on temperature, the average abundance of those ecosystems that do survive shows no temperature response and no sensitivity to interspecific variation in TRC (Fig. 7). Evidence from trees supports our finding that abundance is temperature-independent (Allen et al., 2002). However, data on the thermal response of abundance is lacking (He et al., 2019), partially due to the challenges of defining ecosystem boundaries. Our finding that abundance is temperature-independent differs from the result of Arthur and Nicholson (2023), who also modified the TaNa model to include temperature. Arthur and Nicholson (2023) focus on feedbacks arising when TaNa ecosystems affect temperature in addition to responding to it, but their paper also includes simulations in which species do not modify temperature, and in those simulations abundance scales with the organism-level TRC. The difference between our results arises because Arthur and Nicholson (2023) vary interaction strength scaler (C) with temperature, rather than $p_{off,T}$, p_{death} and p_{mut}. Abundance is affected by C in the TaNa model because in a steady state, $p_{off,total} \approx p_{death}$, leading to $N \approx \frac{1}{\mu}\left[\log(\frac{p_{death}}{p_{off,T}} - 1) + \sum_j \left(J_{ij}\frac{N_j}{N}\right)\right]$. The first term in the parentheses is small, whereas the second term can be on the order of C, here set to 100, making C (in addition to μ) the dominant parameters controlling abundance (also see Fig. Fig. C.12). In our study, holding C and μ constant enabled us to test how ecosystem characteristics evolve in response to physiological TRC alone. Our result that reproduction, death, and mutation rates do not affect ecosystem abundance provides a helpful addition to MTE predictions, and clearly distinguishes the thermal response of abundance from that of species populations.

We find that species richness increases exponentially with increasing temperature, as predicted by MTE (Allen et al., 2002; Price et al., 2010), with or without interspecific variation in TRC (Fig. 7 c,d). The temperature-dependence of species richness is driven by temperature-dependence of mutation rate (Fig. 4). In a similar model, Stegen et al. (2009) found that species richness loses its temperature-dependence over time; a result we do not reproduce. The discrepancy in results from the two models probably arises because Stegen et al. (2009) allow mutation rates to vary between species at the same temperature (depending on species' bodymass), whereas we keep mutation probability the same for all species at the same temperature. An intriguing direction of future study would be to test the effect of interspecific variation in mutation rates in the TaNa+T to confirm whether a time-decaying temperature-dependence of species richness would arise. The relationship between interspecific variation in mutation rates and species richness could also help explain the persistence of a latitudinal biodiversity gradient, since it is usually measured for related species, which may have quite similar sizes and thus less interspecific variation in mutation rate.

Average species richness of core species increases with temperature in the TaNa+T as well, but more gradually than the overall species richness and with a smaller activation energy than that of metabolism (Fig. 7 i,j). In other words, the richness of the most abundant species is less sensitive to temperature than the richness of rare species. These results should also be considered in the context of the latitudinal diversity gradient.

The different thermal-dependencies of species richness for core and cloud species drives a temperature-dependent effect on Species Abundance Distributions (SADs) in the TaNa+T, with a larger proportion of rare species in warmer populations (Fig. 8). SADs are one of the few ecological properties to have a "universal" shape, but the mechanisms generating this shape, and the factors controlling differences like SAD skewness, remain poorly understood (McGill et al., 2007). Previously, SAD skewness has been associated with species richness, but we find that temperature is the primary driver of SAD skewness (Fig. 9). Additionally, while species richness affects SAD skewness for ecosystems of

the same temperature in various-TRC experiments, it has no effect on SAD skewness in single-TRC experiments (Fig. 9). These findings can advance our understanding of "universal laws" in ecology.

Interaction strengths are more positive in cold temperatures and become increasingly neutral in warmer temperatures in the TaNa+T (Fig. 10). Because some empirical studies indicated that the rates of activities related to interactions increase in proportion to the Arrhenius equation (Dell et al., 2011), we tested whether an exponential increase in TaNa interaction strengths could arise secondarily to the more basic physiological TRC. However, our results show that interactions are inversely related with the Arrhenius curve, which implies that an exponential increase in interaction strengths is not a higher-level response to physiological TRC. Future work could consider the effect of simultaneously varying mutation and interaction strength scaler (C) with temperature, and determine which TRC would have a stronger effect on the evolution of interactions between species. Additionally, the relationship between interaction strength and abundance — which varies with C in the TaNa model — could be further investigated.

The TaNa+T model isolates a few components of ecological complexity, but many more layers of complexity remain to be disentangled. For example, interspecific variation in other TRC probably affects other ecosystem thermal responses (Stegen et al., 2009; Bideault et al., 2021). The width of TRC may also vary between species (TRC width may be correlated with latitude; Amarasekare and Savage (2012), predator–prey relationships; Dell et al. (2011), or climate variability; Chen et al. (2022)). Additionally, there may be constraints on the ways that TRC can vary between species; for example, MTE predicts that TRC peak height is controlled by metabolic rate (Gillooly et al., 2001; Brown et al., 2004; Chen, 2022). Another particularly interesting direction of future research is the feedback that could arise through biotic effects on the climate (Wilkinson, 2006; Arthur and Nicholson, 2023), and the ways in which ecological complexity affects it.

6. Conclusions

Here we have pieced together three fundamental ways species respond to temperature and extrapolated them to ecosystem-level outcomes in the TaNa+T model. In this model, we modify the TaNa model of ecology and evolution by making reproduction, death, and mutation probabilities temperature-dependent, allowing us to investigate how these physiological Thermal Response Curves (TRC) can create ecosystem-level thermal responses. We find that ecosystem survival probability, species richness, Species Abundance Distributions (SADs), and interactions all respond to temperature via physiological TRC, while mean abundance of surviving ecosystems, interaction types, and connectance do not. Even when all species have the same TRC, ecosystem properties do not always have the same thermal responses as species-level TRC, and not all ecosystem metrics respond to the same underlying TRC. Additionally, while it has been suspected that thermal diversity may diminish ecosystem-level thermal responses, we find that interspecific variation in the optimal temperature of reproduction only affects the thermal response of ecosystem survival probability.

This work helps clarify how thermal responses propagate from molecular to ecological scales according to the Metabolic Theory of Ecology (MTE). We show that mutation alone can drive the thermal responses of species richness, population sizes, and interaction strengths. However, mutation affects interactions inversely to what was previously expected; causing interactions to decrease from positive to more neutral as temperature increases. This study additionally highlights the importance of a relatively uncommon thermal response, ecosystem survival probability, which may also be important in the thermal response of abundance. Controlling for ecosystem survival probability, abundance shows no thermal response. We emphasize the distinction between the thermal responses of abundance and population size, which have sometimes been considered interchangeably in the past, but which respond very differently to temperature in the TaNa+T. Overall, understanding how ecosystems respond to the environment at a coarse level can provide a baseline from which to investigate the variety and complexity of ecology. We hope this work contributes to clarifying how TRC scale up in the theory of MTE and in ecology in general.

CRediT authorship contribution statement

Camille Febvre: Conceptualization, Formal analysis, Investigation, Methodology, Software, Visualization, Writing – original draft, Writing – review & editing. **Colin Goldblatt:** Conceptualization, Funding acquisition, Supervision, Writing – review & editing. **Rana El-Sabaawi:** Conceptualization, Funding acquisition, Supervision, Writing – review & editing.

Declaration of competing interest

The authors declare that they have no known competing financial interests or personal relationships that could have appeared to influence the work reported in this paper.

Data and code availability

The TaNa+T model and plotting scripts are available in a public git repository: https://github.com/camille-e-e/TaNa-T.git. Model output is publicly available in a Federated Research Data Repository: "Thermal response of the Tangled Nature Model + Temperature" (Febvre, C., 2024), https://doi.org/10.20383/103.0924.

Acknowledgments

We are sincerely grateful for invaluable input from Dr. Carsten Abraham throughout this process, including advice on model design, implementation, and interpretation, and editing of the manuscript. We would also like to thank the two anonymous reviewers whose insightful input and suggestions improved the formulation of the work presented here. Financial support for this research was provided by the Natural Sciences and Engineering Research Council of Canada (NSERC) through Discovery Grants RGPIN-2018-05929 to Colin Goldblatt, and 2020-06495 to Rana El-Sabaawi. High Performance computing resources were provided through NSERC Research Tools and Equipment Grant RTI-2020-00277. We do not have any conflict of interest to declare.

Appendix A. Example TaNa model output

The first 4000 generations of 4 TaNa model simulations are shown in Fig. A.11.

Appendix B. Parameters used in reproduction TRC

Reproduction rate (r_{off}) in the TaNa+T is approximated with a left-skew normal curve such that the shape of the skew-normal curve matches the second term in Eq. 11 in Amarasekare and Savage (2012). That equation gives a general TRC derived from temperature-dependence of fecundity (the reproduction rate of an individual), development (the rate at which fecundity changes with an organism's age) and mortality (Amarasekare and Savage, 2012). The TRC of reproduction rate is defined as

$$r_{\text{off}}(T) = \frac{1}{\alpha(T)} W\left[b_{\alpha_{\text{peak}}}(T)\alpha(T) \exp\left[\left(r_{\text{death}}(T) - r_{\text{death,juv}}(T)\right)\alpha(T)\right]\right], \tag{B.1}$$

where T is temperature, $\alpha(T)$ is age at first reproduction, $W(\cdot)$ is the Lambert W function (arising in the solution to the temperature-dependence of the Euler–Lotka equation for fecundity), $b_{\alpha_{\text{peak}}}(T)$ is

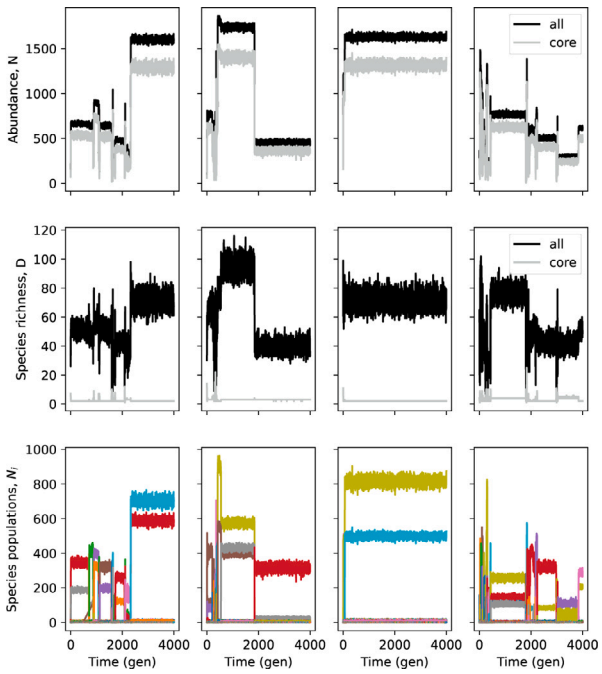

Fig. A.11. Each column shows a single TaNa model simulation for its first 4000 generations. Rows illustrate ecosystem characteristics; from top to bottom: 1. abundance (number of individuals) in ecosystems (black) and cores (gray); 2. species richness (number of species); and 3. populations of each species (colors).

Table B.2
Parameter values used for Eqs. (B.1) & (6) (Fig. 1 birth rate: black solid line, death rate: gray solid line).

Parameters for reproduction and mortality rates		
A_a	Activation energy of development	−8000 eV
$A_{d,j}$	Activation energy of death of juveniles	7500 eV
A_d	Activation energy of death of adults	6000 eV
α_{T_r}	Development rate at T_r	60
b_{T_r}	Birth rate at T_r	50
$\bar{b}_{T_r}$	Average birth rate at T_r	295
d_{j,T_r}	Death rate of juveniles at T_r	0.03
d_{T_r}	Death rate of adults at T_r	0.05
T_r	Reference temperature	294 K
T_{opt}	Optimum temperature for reproduction	298 K

maximum fecundity (expected number of offspring at the age of first reproduction, assuming fecundity decreases thereafter), and $r_{death}(T)$ and $r_{death,juv}(T)$ are death rates of adults and juveniles, respectively ($r_{off}(T)$ and $r_{death}(T)$ shown as solid black and gray lines, respectively, in Fig. 1). Development and mortality are modeled as Boltzmann–Arrhenius exponential equations, and fecundity is given a Gaussian shape (Amarasekare and Savage, 2012). The parameters we used in Eq. (B.1) are listed in Table B.2.

Appendix C. 1-D exploration of all 7 TaNa parameters

C.1. Testing ecological sensitivity to tana model parameters

We varied each of the 7 TaNa model parameters along one dimension (holding all other parameters constant) in 50 simulations at each parameterization. Ecosystem survival probability, abundance, species richness, and core species richness are measured after 10,000 generations (Fig. C.12).

Ecosystem survival probability is sensitive to 4 of the 7 parameters: temperature-dependent scaler of reproduction probability ($p_{off,T}$), death probability (p_{death}), mutation probability (p_{mut}), and damping factor of carrying capacity (μ) (Fig. C.12, top row). Ecosystem survival decreases from 1 to 0 as $p_{off,T}$ decreases or p_{death} increases. For values of p_{mut} greater than the control value (0.01 mutations per gene per timestep), survival remains near 1, but decreases toward 0.8 for p_{mut} values below that. Survival also decreases for values of μ greater than the control (0.1), which are associated with relatively small carrying capacities (less than about 700 individuals, Fig. C.12) and species richness less than about 60. The other parameters do not affect survival probability for the range of parameter values sampled.

Abundance is sensitive to μ and interaction strength scaler (C) (Fig. C.12, second row). μ scales the carrying capacity of the model, so its effect on abundance is expected. C affects the fitness equation, Eq. (3), by scaling the positive term, so increasing C has the same effect as decreasing μ, and it is therefore not surprising that these two parameters have similar effects on the model. No other parameter affects abundance in the TaNa model.

Species richness is affected by p_{mut}, μ, and genome length (L) (Fig. C.12, third row). Increasing mutation rate enables more species to enter the model per unit time, contributing to a larger equilibrium species richness. Increasing L has a similar effect as increasing p_{mut}, because each individual gets L chances for a mutation to occur during reproduction. Increasing μ does not affect speciation rate but enables more individuals to coexist in the model, and thereby allows more different species to coexist.

Core species richness responds only to p_{mut} (Fig. C.12, bottom row). This is interesting because even though μ increases abundance and species richness, it does not affect the number of stable core species — only the number of cloud species.

C.2. Temperature dependence of TaNa model parameters

The three physiological parameters in the TaNa model (birth, death, and mutation probabilities) reflect intrinsic, organism-level rates which are all predicted to increase exponentially with temperature according to the Arrhenius curve due to their dependence on metabolic rate (Gillooly et al., 2001; Brown et al., 2004; Gillooly et al., 2005). We vary these three rates with temperature in the TaNa+T model, and keep the other parameters constant in order to test how physiological properties propagate upward through ecological networks. However, some discussion of the temperature dependencies of the other parameters is warranted.

Interaction strength is not explicitly encompassed by MTE, but some empirical measures of activities associated with interaction strength or trophic interactions, such as attack or escape velocity, increase with temperature according to the Boltzmann–Arrhenius equation (Dell et al., 2011). Network connectance (θ) was also found to increases in warmer temperatures in some studies (Yuan et al., 2021). However, for both interaction scale and network connectance, the connection between individual physiology and traits affecting these network-level characteristics is not obvious. We choose to test whether either response may emerge secondarily from other physiological TRC, rather than being direct physiological responses to temperature themselves.

Carrying capacity (scaled by μ) could vary with temperature for a number of reasons. For example, productivity could be higher in warmer or more optimal temperatures, or the temperature-dependence of nutrient recycling by microbes could affect nutrient availability (either positively or negatively). On weathering timescales, primary nutrients come from weathering bedrock, and weathering rates generally increase in warmer climates (Berner, 1990). Future research should continue to investigate the responses of resource availability to temperature, but currently, it is standard in MTE not to assume that resources vary with temperature, and empirical patterns seen in trees support this prediction (Allen et al., 2002; Brown et al., 2004).

The last parameter in the TaNa model is genome length (L), and we do not know of any evidence that L is affected by temperature. However, Stegen et al. (2009) assume that genome length increases

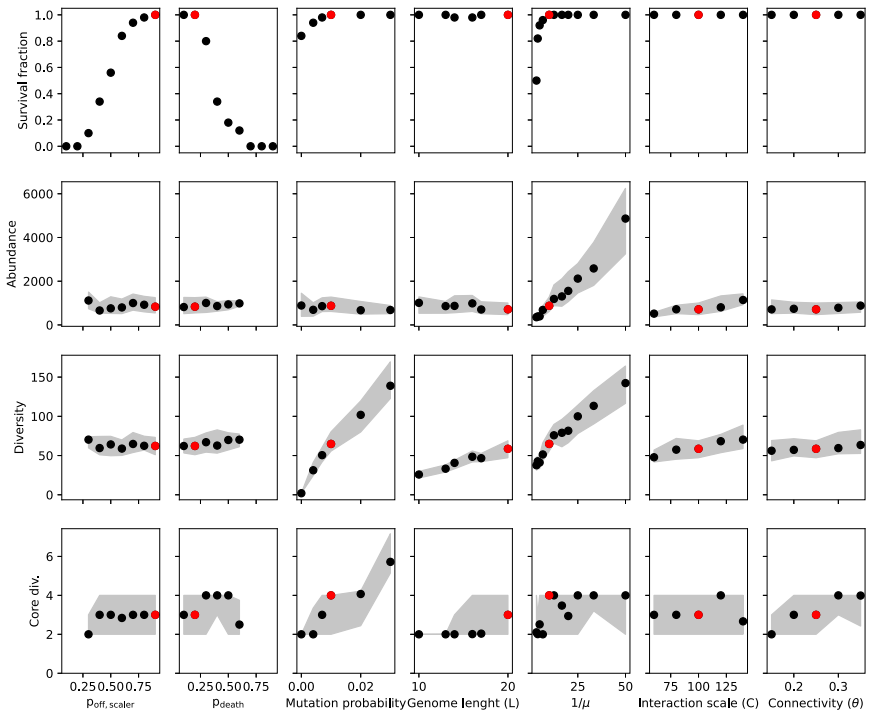

Fig. C.12. Seven TaNa model parameters are varied independently while holding all values constant. The first column shows how reproduction probability was scaled ($p_{\mathrm{off,T}}$), which is a parameter we introduce to scale ecological reproduction probability ($p_{\mathrm{off,f}}$, Eq. (2)). The other six columns show variation of the six intrinsic TaNa model parameters: death probability (p_{death}), mutation probability (p_{mut}), genome length (L), carrying capacity scaler ($\frac{1}{\mu}$), interaction scale (C), and connectance (θ). Each dot corresponds to 50 experiments: in the top row, the fraction of those 50 experiments that survived for 10,000 generations is shown, and for the other rows, the dot sows the median and the shaded gray region shows the interquartile range. The red dots in all plots indicate the control value of the parameter.

with mass (which they deem a rough approximation) in their eco-evolutionary model of MTE. As their model (like the Tana model) utilizes per-gene mutation rates, increasing L has the effect of increasing the mutation rates of larger organisms in their model. Here, we do not treat mass, and to keep the complexity to a minimum in our model, we hold genome length constant for organisms in our model. However, varying genome length between model species could be an interesting area of further investigation.

References

Allen, A.P., Brown, J.H., Gillooly, J.F., 2002. Global biodiversity, biochemical kinetics, and the energetic-equivalence rule. Science 297 (5586), 1545–1548. http://dx.doi.org/10.1126/science.1072380, URL: https://www.science.org/doi/full/10.1126/science.1072380. Publisher: American Association for the Advancement of Science.

Allsup, C.M., George, I., Lankau, R.A., 2023. Shifting microbial communities can enhance tree tolerance to changing climates. Science 380 (6647), 835–840. http://dx.doi.org/10.1126/science.adf2027, URL: https://www.science.org/doi/full/10.1126/science.adf2027. Publisher: American Association for the Advancement of Science.

Amarasekare, P., Savage, V., 2012. A framework for elucidating the temperature dependence of fitness.. Amer. Nat. 179 (2), 178–191. http://dx.doi.org/10.1086/663677, URL: http://www.journals.uchicago.edu/doi/full/10.1086/663677. Publisher: The University of Chicago Press.

Anderson, P.E., Jensen, H.J., 2005. Network properties, species abundance and evolution in a model of evolutionary ecology. J. Theoret. Biol. 232 (4), 551–558. http://dx.doi.org/10.1016/j.jtbi.2004.03.029, URL: https://www.sciencedirect.com/science/article/pii/S0022519304004229.

Arroyo, J.I., Diez, B., Kempes, C.P., West, G.B., Marquet, P.A., 2022. A general theory for temperature dependence in biology | PNAS. Proc. Natl. Acad. Sci. USA 119 (3).

Arthur, R., Nicholson, A., 2023. A gaian habitable zone. Mon. Not. R. Astron. Soc. 521 (1), 690–707. http://dx.doi.org/10.1093/mnras/stad547, URL: arXiv:2301.02150 [astro-ph, q-bio].

Arthur, R., et al., 2017. Tangled nature model for organizational ecology.

Bailey, N.W., 2012. Evolutionary models of extended phenotypes. Trends Ecol. Evol. 27 (10), 561–569. http://dx.doi.org/10.1016/j.tree.2012.05.011, URL: https://www.sciencedirect.com/science/article/pii/S0169534712001267.

Berner, R.A., 1990. Atmospheric carbon dioxide levels over phanerozoic time. Science 249 (4975), 1382–1386. http://dx.doi.org/10.1126/science.249.4975.1382, URL: https://www.sciencemag.org/lookup/doi/10.1126/science.249.4975.1382.

Bideault, A., Galiana, N., Zelnik, Y.R., Gravel, D., Loreau, M., Barbier, M., Sentis, A., 2021. Thermal mismatches in biological rates determine trophic control and biomass distribution under warming. Global Change Biol. 27 (2), 257–269. http://dx.doi.org/10.1111/gcb.15395, URL: https://onlinelibrary.wiley.com/doi/abs/10.1111/gcb.15395. _eprint: https://onlinelibrary.wiley.com/doi/pdf/10.1111/gcb.15395.

Braghiere, R.K., Quaife, T., Black, E., He, L., Chen, J.M., 2019. Underestimation of global photosynthesis in earth system models due to representation of vegetation structure. Glob. Biogeochem. Cycles 33 (11), 1358–1369. http://dx.doi.org/10.1029/2018GB006135, URL: http://onlinelibrary.wiley.com/doi/abs/10.1029/2018GB006135, _eprint: https://agupubs.onlinelibrary.wiley.com/doi/pdf/10.1029/2018GB006135.

Brodie, J.F., Mannion, P.D., 2022. The hierarchy of factors predicting the latitudinal diversity gradient. Trends Ecol. Evol. http://dx.doi.org/10.1016/j.tree.2022.07.013, URL: https://www.sciencedirect.com/science/article/pii/S0169534722001951.

Brown, J.H., Gillooly, J.F., Allen, A.P., Savage, V., West, G.B., 2004. Toward a metabolic theory of ecology. Ecology 85 (7), 1771–1789. http://dx.doi.org/10.1890/03-9000, URL: http://onlinelibrary.wiley.com/doi/abs/10.1890/03-9000. _eprint: https://esajournals.onlinelibrary.wiley.com/doi/pdf/10.1890/03-9000.

Butchart, S.H.M., Walpole, M., Collen, B., van Strien, A., Scharlemann, J.P.W., Almond, R.E.A., Baillie, J.E.M., Bomhard, B., Brown, C., Bruno, J., Carpenter, K.E., Carr, G.M., Chanson, J., Chenery, A.M., Csirke, J., Davidson, N.C., Dentener, F., Foster, M., Galli, A., Galloway, J.N., Genovesi, P., Gregory, R.D., Hockings, M., Kapos, V., Lamarque, J.-F., Leverington, F., Loh, J., McGeoch, M.A., McRae, L., Minasyan, A., Morcillo, M.H., Oldfield, T.E.E., Pauly, D., Quader, S., Revenga, C., Sauer, J.R., Skolnik, B., Spear, D., Stanwell-Smith, D., Stuart, S.N., Symes, A., Tierney, M., Tyrrell, T.D., Vié, J.-C., Watson, R., 2010. Global biodiversity: Indicators of recent declines. Science 328 (5982), 1164–1168. http://dx.doi.org/10.1126/science.1187512, URL: https://www.science.org/doi/full/10.1126/science.1187512. Publisher: American Association for the Advancement of Science.

Chen, B., 2022. Thermal diversity affects community responses to warming. Ecol. Model. 464, 109846. http://dx.doi.org/10.1016/j.ecolmodel.2021.109846, URL: https://www.sciencedirect.com/science/article/pii/S0304380021003847.

Chen, H., Jing, Q., Liu, X., Zhou, X., Fang, C., Li, B., Zhou, S., Nie, M., 2022. Microbial respiratory thermal adaptation is regulated by r-/K-strategy dominance. Ecol. Lett. n/a (n/a), http://dx.doi.org/10.1111/ele.14106, URL: http://onlinelibrary.wiley.com/doi/abs/10.1111/ele.14106. _eprint: https://onlinelibrary.wiley.com/doi/pdf/10.1111/ele.14106.

Christensen, K., Di Collobiano, S.A., Hall, M., Jensen, H.J., 2002. Tangled nature: A model of evolutionary ecology. J. Theoret. Biol. 216 (1), 73–84. http://dx.doi.org/10.1006/jtbi.2002.2530, URL: https://linkinghub.elsevier.com/retrieve/pii/S0022519302925300.

Cowie, R.H., Bouchet, P., Fontaine, B.t., 2022. The sixth mass extinction: fact, fiction or speculation? Biol. Rev. 97 (2), 640–663. http://dx.doi.org/10.1111/brv.12816, URL: https://onlinelibrary.wiley.com/doi/abs/10.1111/brv.12816. _eprint: https://onlinelibrary.wiley.com/doi/pdf/10.1111/brv.12816.

Day, R.L., Laland, K.N., Odling-Smee, F.J., 2003. Rethinking adaptation: The Niche-construction perspective. Perspect. Biol. Med. 46 (1), 80–95. http://dx.doi.org/10.1353/pbm.2003.0003, URL: http://muse.jhu.edu/article/38634. Publisher: Johns Hopkins University Press.

Dell, A.I., Pawar, S., Savage, V., 2011. Systematic variation in the temperature dependence of physiological and ecological traits. Proc. Natl. Acad. Sci. USA 108 (26), http://dx.doi.org/10.1073/pnas.1015178108, URL: http://www.pnas.org/doi/10.1073/pnas.1015178108.

Eichenseer, K., Balthasar, U., Smart, C.W., Stander, J., Haaga, K.A., Kiessling, W., 2019. Jurassic shift from abiotic to biotic control on marine ecological success. Nat. Geosci. 12 (8), 638–642. http://dx.doi.org/10.1038/s41561-019-0392-9, URL: http://www.nature.com/articles/s41561-019-0392-9. Bandiera_abtest: a Cg_type: Nature Research Journals Number: 8 Primary_atype: Research Publisher: Nature Publishing Group Subject_term: Biogeochemistry;Carbon cycle;Ecology;Evolutionary ecology;Palaeoecology Subject_term_id: biogeochemistry;carbon-cycle;ecology;evolutionary-ecology;palaeoecology.

Ezard, T.H.G., Aze, T., Pearson, P.N., Purvis, A., 2011. Interplay between changing climate and species' ecology drives macroevolutionary dynamics | science. Science 332 (6027), 349–351. http://dx.doi.org/10.1126/science.1203060, URL: https://www-science-org.ezproxy.library.uvic.ca/doi/full/10.1126/science.1203060.

Farrell, A.P., 2016. Pragmatic perspective on aerobic scope: peaking, plummeting, pejus and apportioning. J. Fish Biol. 88 (1), 322–343. http://dx.doi.org/10.1111/jfb.12789, URL: https://onlinelibrary.wiley.com/doi/abs/10.1111/jfb.12789. _eprint: https://onlinelibrary.wiley.com/doi/pdf/10.1111/jfb.12789.

Gillooly, J.F., Allen, A.P., West, G.B., Brown, J.H., 2005. The rate of DNA evolution: Effects of body size and temperature on the molecular clock. Proc. Natl. Acad. Sci. 102 (1), 140–145. http://dx.doi.org/10.1073/pnas.0407735101, URL: https://www.pnas.org/doi/abs/10.1073/pnas.0407735101. Publisher: Proceedings of the National Academy of Sciences.

Gillooly, J.F., Brown, J.H., West, G.B., Savage, V., Charnov, E.L., 2001. Effects of size and temperature on metabolic rate. Science 293 (5538), 2248–2251. http://dx.doi.org/10.1126/science.1061967, URL: https://www.science.org/doi/10.1126/science.1061967.

Gould, S.J., Eldredge, N., 1977. Punctuated equilibria: the tempo and mode of evolution reconsidered. Paleobiology 3 (2), 115–151. http://dx.doi.org/10.1017/S0094837300005224, URL: http://www.cambridge.org/core/journals/paleobiology/article/abs/punctuated-equilibria-the-tempo-and-mode-of-evolution-reconsidered/416469B94B074D3F7311C805274679D4. Publisher: Cambridge University Press.

Griffin, C.T., Wynd, B.M., Munyikwa, D., Broderick, T.J., Zondo, M., Tolan, S., Langer, M.C., Nesbitt, S.J., Taruvinga, H.R., 2022. Africa's oldest dinosaurs reveal early suppression of dinosaur distribution | Nature. Nature http://dx.doi.org/10.1038/s41586-022-05133-x, URL: https://www.nature.com/articles/s41586-022-05133-x.

Guimarães, P.R., Pires, M.M., Jordano, P., Bascompte, J., Thompson, J.N., 2017. Indirect effects drive coevolution in mutualistic networks. Nature 550 (7677), 511–514. http://dx.doi.org/10.1038/nature24273, URL: https://www.nature.com/articles/nature24273. Number: 7677 Publisher: Nature Publishing Group.

He, N., Liu, C., Piao, S., Sack, L., Xu, L., Luo, Y., He, J., Han, X., Zhou, G., Zhou, X., Lin, Y., Yu, Q., Liu, S., Sun, W., Niu, S., Li, S., Zhang, J., Yu, G., 2019. Ecosystem traits linking functional traits to macroecology. Trends Ecol. Evol. 34 (3), 200–210. http://dx.doi.org/10.1016/j.tree.2018.11.004, URL: https://www.cell.com/trends/ecology-evolution/abstract/S0169-5347(18)30275-1. Publisher: Elsevier.

Huete-Stauffer, T.M., Arandia-Gorostidi, N., Díaz-Pérez, L., Morán, X.A.G., 2015. Temperature dependences of growth rates and carrying capacities of marine bacteria depart from metabolic theoretical predictions. FEMS Microbiol. Ecol. 91 (10), fiv111. http://dx.doi.org/10.1093/femsec/fiv111.

Irlich, U.M., Terblanche, J.S., Blackburn, T.M., Chown, S.L., 2009. Insect rate-temperature relationships: Environmental variation and the metabolic theory of ecology. Amer. Nat. 174 (6), 819–835. http://dx.doi.org/10.1086/647904, URL: http://www.journals.uchicago.edu/doi/full/10.1086/647904. Publisher: The University of Chicago Press.

Isaac, N.J.B., Carbone, C., McGill, B., 2012. Population and community ecology. In: Metabolic Ecology. John Wiley & Sons, Ltd, pp. 77–85. http://dx.doi.org/10.1002/9781119968535.ch7, URL: http://onlinelibrary.wiley.com/doi/abs/10.1002/9781119968535.ch7. Section 7 _eprint: https://onlinelibrary.wiley.com/doi/pdf/10.1002/9781119968535.ch7.

Jones, D.O.B., Yool, A., Wei, C.-L., Henson, S.A., Ruhl, H.A., Watson, R.A., Gehlen, M., 2014. Global reductions in seafloor biomass in response to climate change. Global Change Biol. 20 (6), 1861–1872. http://dx.doi.org/10.1111/gcb.12480, URL: https://onlinelibrary.wiley.com/doi/abs/10.1111/gcb.12480. _eprint: https://onlinelibrary.wiley.com/doi/pdf/10.1111/gcb.12480.

Kordas, R.L., Harley, C.D.G., O'Connor, M.I., 2011. Community ecology in a warming world: The influence of temperature on interspecific interactions in marine systems. J. Exp. Mar. Biol. Ecol. 400 (1), 218–226. http://dx.doi.org/10.1016/j.jembe.2011.02.029, URL: https://www.sciencedirect.com/science/article/pii/S0022098111000773.

Laland, K.N., 2004. Extending the extended phenotype. Biol. Philos. 19 (3), 313–325. http://dx.doi.org/10.1023/B:BIPH.0000036113.38737.d8, URL: http://link.springer.com/10.1023/B:BIPH.0000036113.38737.d8.

Lenton, T., Watson, A.J., 2000. Redfield revisited: 1. regulation of nitrate, phosphate, and oxygen in the ocean. Glob. Biogeochem. Cycles 14 (1), 225–248. http://dx.doi.org/10.1029/1999GB900065, URL: http://onlinelibrary.wiley.com/doi/abs/10.1029/1999GB900065. _eprint: https://agupubs.onlinelibrary.wiley.com/doi/pdf/10.1029/1999GB900065.

Lewontin, R., Levins, R., 1997. Organism and environment. Capitalism Nature Socialism 8 (2), 95–98. http://dx.doi.org/10.1080/10455759709358737, URL: http://www.tandfonline.com/doi/abs/10.1080/10455759709358737.

Loeuille, N., Loreau, M., 2005. Evolutionary emergence of size-structured food webs. Proc. Natl. Acad. Sci. 102 (16), 5761–5766. http://dx.doi.org/10.1073/pnas.0408424102, URL: https://www.pnas.org/doi/abs/10.1073/pnas.0408424102. Publisher: Proceedings of the National Academy of Sciences.

McGill, B.J., Enquist, B.J., Weiher, E., Westoby, M., 2006. Rebuilding community ecology from functional traits. Trends Ecol. Evol. 21 (4), 178–185. http://dx.doi.org/10.1016/j.tree.2006.02.002, URL: https://www.cell.com/trends/ecology-evolution/abstract/S0169-5347(06)00033-4. Publisher: Elsevier.

McGill, B.J., Etienne, R.S., Gray, J.S., Alonso, D., Anderson, M.J., Benecha, H.K., Dornelas, M., Enquist, B.J., Green, J.L., He, F., Hurlbert, A.H., Magurran, A.E., Marquet, P.A., Maurer, B.A., Ostling, A., Soykan, C.U., Ugland, K.I., White, E.P., 2007. Species abundance distributions: moving beyond single prediction theories to integration within an ecological framework. Ecol. Lett. 10 (10), 995–1015. http://dx.doi.org/10.1111/j.1461-0248.2007.01094.x, URL: https://onlinelibrary.wiley.com/doi/abs/10.1111/j.1461-0248.2007.01094.x. _eprint: https://onlinelibrary.wiley.com/doi/pdf/10.1111/j.1461-0248.2007.01094.x.

Moorcroft, P.R., 2006. How close are we to a predictive science of the biosphere? Trends Ecol. Evol. 21 (7), 400–407. http://dx.doi.org/10.1016/j.tree.2006.04.009, URL: https://www.sciencedirect.com/science/article/pii/S0169534706001509.

Odling-Smee, F.J., Laland, K.N., Feldman, M., 1996. Niche construction. Amer. Nat. 147 (4), 641–648. http://dx.doi.org/10.1086/285870, URL: http://www.journals.uchicago.edu/doi/epdf/10.1086/285870.

Peters, S.E., Kelly, D.C., Fraass, A.J., 2013. Oceanographic controls on the diversity and extinction of planktonic foraminifera. Nature 493 (7432), 398–401. http://dx.doi.org/10.1038/nature11815, URL: https://www.nature.com/articles/nature11815. Number: 7432 Publisher: Nature Publishing Group.

Price, C.A., Gilooly, J.F., Allen, A.P., Weitz, J.S., Niklas, K.J., 2010. The metabolic theory of ecology: prospects and challenges for plant biology. New Phytol. 188 (3), 696–710. http://dx.doi.org/10.1111/j.1469-8137.2010.03442.x, URL: https://onlinelibrary.wiley.com/doi/abs/10.1111/j.1469-8137.2010.03442.x. _eprint: https://onlinelibrary.wiley.com/doi/pdf/10.1111/j.1469-8137.2010.03442.x.

Qin, W., Chen, Y., Wang, X., Zhao, H., Hou, Y., Zhang, Q., Guo, X., Zhang, Z., Zhu, B., 2022. Whole-soil warming shifts species composition without affecting diversity, biomass and productivity of the plant community in an alpine meadow. Fundamental Res. http://dx.doi.org/10.1016/j.fmre.2022.09.025, URL: https://www.sciencedirect.com/science/article/pii/S2667325822003910.

Remke, M.J., Johnson, N.C., Bowker, M.A., 2022. Sympatric soil biota mitigate a warmer-drier climate for Bouteloua gracilis. Global Change Biol. 28 (21), 6280–6292. http://dx.doi.org/10.1111/gcb.16369, URL: http://onlinelibrary.wiley.com/doi/abs/10.1111/gcb.16369. _eprint: https://onlinelibrary.wiley.com/doi/pdf/10.1111/gcb.16369.

Remolina-Figueroa, D., Prieto-Torres, D.A., Dáttilo, W., Salgado Díaz, E., Nuñez Rosas, L.E., Rodríguez-Flores, C., Navarro-Sigüenza, A.G., Arizmendi, M.d.C., 2022. Together forever? Hummingbird-plant relationships in the face of climate warming. Clim. Change 175 (1), 2. http://dx.doi.org/10.1007/s10584-022-03447-3.

Rezende, E.L., Bozinovic, F., 2019. Thermal performance across levels of biological organization. Philos. Trans. R. Soc. B 374 (1778), 20180549. http://dx.doi.org/10.1098/rstb.2018.0549, URL: https://royalsocietypublishing.org/doi/full/10.1098/rstb.2018.0549. Publisher: Royal Society.

Rosenzweig, C., Karoly, D., Vicarelli, M., Neofotis, P., Wu, Q., Casassa, G., Menzel, A., Root, T.L., Estrella, N., Seguin, B., Tryjanowski, P., Liu, C., Rawlins, S., Imeson, A., 2008. Attributing physical and biological impacts to anthropogenic climate change. Nature 453 (7193), 353–357. http://dx.doi.org/10.1038/nature06937, URL: https://www.nature.com/articles/nature06937. Number: 7193 Publisher: Nature Publishing Group.

Stegen, J.C., Enquist, B.J., Ferriere, R., 2009. Advancing the metabolic theory of biodiversity. Ecol. Lett. 12 (10), 1001–1015. http://dx.doi.org/10.1111/j.1461-0248.2009.01358.x, URL: https://onlinelibrary.wiley.com/doi/abs/10.1111/j.1461-0248.2009.01358.x. _eprint: https://onlinelibrary.wiley.com/doi/pdf/10.1111/j.1461-0248.2009.01358.x.

Strona, G., Bradshaw, C.J.A., 2022. Coextinctions dominate future vertebrate losses from climate and land use change. Sci. Adv. 8 (50), eabn4345. http://dx.doi.org/10.1126/sciadv.abn4345, URL: https://www.science.org/doi/10.1126/sciadv.abn4345. Publisher: American Association for the Advancement of Science.

Tilman, D., HilleRisLambers, J., Harpole, S., Dybzinski, R., Fargione, J., Clark, C., Lehman, C., 2004. Does metabolic theory apply to community ecology? It's a matter of scale. Ecology 85 (7), 1797–1799, URL: https://www.jstor.org/stable/3450345. Publisher: Ecological Society of America.

Tittensor, D.P., Novaglio, C., Harrison, C.S., Heneghan, R.F., Barrier, N., Bianchi, D., Bopp, L., Bryndum-Buchholz, A., Britten, G.L., Büchner, M., Cheung, W.W.L., Christensen, V., Coll, M., Dunne, J.P., Eddy, T.D., Everett, J.D., Fernandes-Salvador, J.A., Fulton, E.A., Galbraith, E.D., Gascuel, D., Guiet, J., John, J.G., Link, J.S., Lotze, H.K., Maury, O., Ortega-Cisneros, K., Palacios-Abrantes, J., Petrik, C.M., du Pontavice, H., Rault, J., Richardson, A.J., Shannon, L., Shin, Y.-J., Steenbeek, J., Stock, C.A., Blanchard, J.L., 2021. Next-generation ensemble projections reveal higher climate risks for marine ecosystems. Nature Clim. Change 11 (11), 973–981. http://dx.doi.org/10.1038/s41558-021-01173-9, URL: https://www.nature.com/articles/s41558-021-01173-9. Number: 11 Publisher: Nature Publishing Group.

Walther, G.-R., 2010. Community and ecosystem responses to recent climate change. Philos. Trans. R. Soc. B 365 (1549), 2019–2024. http://dx.doi.org/10.1098/rstb.2010.0021, URL: http://royalsocietypublishing.org/doi/full/10.1098/rstb.2010.0021. Publisher: Royal Society.

Wilkinson, D.M., 2006. Ecological hypercycles—covering a planet with life. In: Wilkinson, D.M. (Ed.), Fundamental Processes in Ecology: An Earth Systems Approach. Oxford University Press, http://dx.doi.org/10.1093/acprof:oso/9780198568469.003.0005.

Wilkinson, D.M., 2007. Fundamental Processes in Ecology: An earth systems approach. OUP Oxford, Google-Books-ID: PCeQDwAAQBAJ.

Yuan, M.M., Guo, X., Wu, L., Zhang, Y., Xiao, N., Ning, D., Shi, Z., Zhou, X., Wu, L., Yang, Y., Tiedje, J.M., Zhou, J., 2021. Climate warming enhances microbial network complexity and stability. Nature Clim. Change 11 (4), 343–348. http://dx.doi.org/10.1038/s41558-021-00989-9, URL: https://www.nature.com/articles/s41558-021-00989-9. Number: 4 Publisher: Nature Publishing Group.